ELSEVIER

Intrafullerene electron transfers in Sm-containing metallofullerenes: $Sm@C_{2n}$ ($74 \leq 2n \leq 84$)

Toshiya Okazaki,* Kazutomo Suenaga,† Yongfu Lian, Zhennan Gu,‡ and Hisanori Shinohara*

**Department of Chemistry, Nagoya University, Nagoya, Japan*
†Japan Science and Technology Corporation, c/o Department of Physics, Meijo University, Nagoya, Japan
‡Department of Chemistry, Peking University, Beijing People's Republic of China

The electronic properties of Sm-containing metallofullerenes, $Sm@C_{74}$, $Sm@C_{76}$ (I, II), $Sm@C_{78}$, $Sm@C_{80}$, $Sm@C_{82}$ (I, II, III) and $Sm@C_{84}$ (I, II, III), are characterized by UV-Vis-NIR absorption spectroscopy and electron energy-loss spectroscopy (EELS). The UV-Vis-NIR absorption spectra of $Sm@C_{74}$, $Sm@C_{80}$, $Sm@C_{82}$ (I, II, III) and $Sm@C_{84}$ (I, II) are quite similar to those of the corresponding Ca, Sr, Ba, Eu, Tm, Yb-based metallofullerenes. In contrast, the absorption spectra of $Sm@C_{76}$ (I, II), $Sm@C_{78}$ and $Sm@C_{84}$(III) show a novel feature: the onset for $Sm@C_{78}$ is observed ~2600 nm, which corresponds to a small band gap (~0.5 eV). Furthermore, the oxidation states of Sm atom in the various fullerene cages are investigated by EELS, which reveals that the Sm atom takes +2 oxidation state in the fullerene cages. A probable rationale for the tendency to have the Sm^{2+} state is presented based on a simple thermochemical cycle model.

INTRODUCTION

Even though Eiji Osawa [1] made the first theoretical prediction on the presence and the stability of the soccer-ball-shaped molecule as early as 1970, it took 15 years for this fascinating molecule to be experimentally detected in a supersonic cluster beam in 1985.[2] During this 15 years period, virtually nobody took care of this molecule. With the advent of macroscopic production of C_{60} and C_{70} in 1990,[3] however, a large number of fullerenes of various sizes and endohedral metallofullerenes[4] have so far been produced, isolated, and characterized. In particular, endohedral metallofullerenes have been known as a novel class of fullerene-related materials, in which 1–4 metal atoms are trapped in the inner hollow space of fullerenes.[4]

One of the most interesting aspects in the metallofullerenes resides in a control of the electronic properties by changing the encapsulated atoms and the fullerene cages. Sm atom is suited for this purpose because the Sm ion can take two oxidation states, i.e., +2 and +3. However, due to the relatively low production efficiency, Sm-containing metallofullerenes have not yet been isolated.

Recently, Lian et al. reported a new DC arc discharge method for increasing the production yield of metallofullerenes by using an alloy/graphite composite rod as an anode.[5–7] This method allows us to produce and isolate various Sm-containing metallofullerenes in macroscopic amounts and to investigate their novel electronic properties.

Here we report a first systematic study on electronic properties of Sm-containing metallofullerenes [$Sm@C_{74}$, $Sm@C_{76}$ (I, II), $Sm@C_{78}$, $Sm@C_{80}$, $Sm@C_{82}$ (I, II, III) and $Sm@C_{84}$ (I, II, III)] by absorption spectroscopy and electron energy-loss spectroscopy (EELS), together with the details of high-performance liquid chromatography isolation schemes. The observed spectroscopic features in the UV-vis-NIR absorption spectra show a similarity to those of Ca, Ba, Sr, Eu, and Tm metallofullerenes. In the EELS spectra, the Sm M_{45} edges of Sm-containing metallofullerenes are shifted by ~2 eV from those of trivalent Sm^{3+} in Sm_2O_3, indicating that Sm has a +2 oxidation state in the fullerene cages. These results are interpreted based on a simple thermochemical cycle model.

METHODS

Details of the synthesis of the soot-containing Sm metallofullerenes are described elsewhere.[6,7] Briefly, the soot was produced with the DC arc discharge method by using a Sm

Corresponding author: Hisanori Shinohara, Department of Chemistry, Nagoya University, Furo-cho, Chikusa-ku, Nagoya 464-8602, Japan. Tel: ++81-(0)52-789-2482; fax: ++81-(0)52-789-2962.

E-mail address: nori@nano.chem.nagoya-u.ac.jp (H. Shinohara)

Journal of Molecular Graphics and Modelling 19, 244–251, 2001

655 Avenue of the Americas, New York, NY 10010

1093-3263/01/$–see front matter
PII S1093-3263(00)00093-0

alloy/graphite composite rod. The arc discharge was carried out under optimized conditions with high He pressures, low electric current, and a wide electrode gap. The soot produced was collected under N_2 atmosphere and extracted by refluxing with CS_2 and pyrizine. The extracts were first chromatographed on silica gel to roughly remove the empty fullerenes.

Each Sm-containing metallofullerene was separated by the multi-step HPLC method (LC-908-C60; Japan Analytical Industry, Tokyo, Japan) using a Buckyprep ($\phi = 20 \times 250$ mm; Nakalai Tesque, Kyoto, Japan) and a Buckyclutcher ($\phi = 21 \times 500$ mm; Regis Chemical, Morton Grove, IL, USA) column.[8] The purity of the isolated Sm fullerenes was determined to be >99 % by LD-TOF-MS spectroscopy (Kompact MALDI-4 Shimadzu / Kratos, Kyoto, Japan). The purity of Sm@C_{76}(II) was found to be slightly lower (>80%).

EELS measurements were carried out under a transmission electron microscope (JEOL 2010F, Tokyo, Japan) operated at 120 kVand 200 kV.[9] The specimen was prepared by putting a few droplets of Sm metallofullerene/CS_2 solution on a perforated carbon micro-grid. The Sm metallofullerene was immediately dried in the TEM chamber ($\sim 10^{-7}$ Torr). The EELS signals were recorded by an electron spectrometer with a CCD-based detector (Gatan Imaging Filter, Gatan, Pleasanton, CA, USA). Great care was taken to prevent contaminant electron irradiation damage during the valence state measurements. A small condenser aperture (20μm) was used to reduce the total current in the incident electron beam, and the region of interest ($\sim$30 nm) was chosen by the smallest area aperture. The electron beam was, therefore, not necessarily tightly focused. Under such conditions, the Sm M_{45} near-edge structure can be recorded with sufficient counting statistics with virtually no irradiation damage. Spectral evolution for the overdosed specimen (more than 60 s acquisition time) has been discussed elsewhere.[10]

The third electron affinities ($E_a(C_{2n}{}^{3-})$) of various fullerene cages were obtained by semi-empirical calculation (PM3) with the Gaussian 98 program package.[11]

RESULTS AND DISCUSSION

Isolation of Sm-metallofullerenes

Details of purification and isolation of metallofullerenes have been reported previously.[8] In the first HPLC stage, we roughly separated Sm-containing metallofullerenes by using a Buckyprep column (12 ml/min flow rate, toluene eluent).[12] Sm@C_{74}, Sm@C_{76} (I, II), and Sm@C_{78} were present in the onset of the fraction, which contained the hollow C_{82} and C_{84} fullerenes.[12] This HPLC elution behavior is consistent with a previous result.[13] Further separation of Sm@C_{74}, Sm@C_{76}(I, II), and Sm@C_{78} was carried out by using the same column (stage 2). After 6 cycles of this fraction, Sm@C_{76}(I) and Sm@C_{78} were isolated. Sm@C_{74} and Sm@C_{76}(II) co-eluted with the empty C_{80}. These species were fully separated by recycling 4 times on a Buckyclutcher column (10 ml/min flow rate, toluene eluent) (stage 3).

The isolation procedures for the other Sm-containing metallofullernes are similar to those of group 2 (Ca, Ba, Sr) metallofullerenes[8,14–19], except for Sm@C_{84}(III).[12] For example, Sm@C_{84}(I, II) eluted in a shoulder on the C_{86} peak (stage 1).[12] In the second stage, we separated Sm@C_{84}(I, II) from the hollow fullerenes (C_{84} and C_{86}) and Sm@C_{80} by using the Buckyclutcher column (10 ml/min flow rate, toluene eluent). After recycling the fraction, Sm@C_{84}(I) and (II) showed different retention times and thus partially separated (Figure 1). Complete separation was achieved by repeating this treatment.

For a qualitative understanding of the relative abundance of Sm fullerenes, we roughly estimate it based on HPLC analysis (Table 1). Out of the Sm metallofullrenes isolated, Sm@C_{74}, Sm@C_{82}(II), and Sm@C_{84}(III) were the most abundant species.

UV-Vis-NIR Absorption Spectroscopy

The UV-Vis-NIR absorption spectrum of Sm@C_{74} (Figure 2a) shows characteristic sharp peaks between 500 and 1000 nm, which are remarkably similar to those of Eu@C_{74}.[20] Dunsch et al. reported UV-Vis-NIR, IR/Raman, EPR, and cyclic voltammetry studies on Eu@C_{74} and suggested that the encapsulated Eu atom takes the oxidation state of +2 and that the plausible structure of the C_{74} cage has D_{3h} symmetry.[20] Since the absorption spectrum is very sensitive to the electronic and geometric structures of the fullerene cage, the spectral similarity suggests that the oxidation state of Sm in Sm@C_{74} is +2 and the C_{74} cage has D_{3h} symmetry.

The absorption spectra of Sm@C_{76}(I, II) are shown in Figure 2b. This is the first isolation of C_{76}-based (and C_{78}-based) metallofullerenes. The absorption spectra of the two isomers of Sm@C_{76} have quite different spectral features. For example, the absorption spectrum of isomer I shows pronounced peaks at

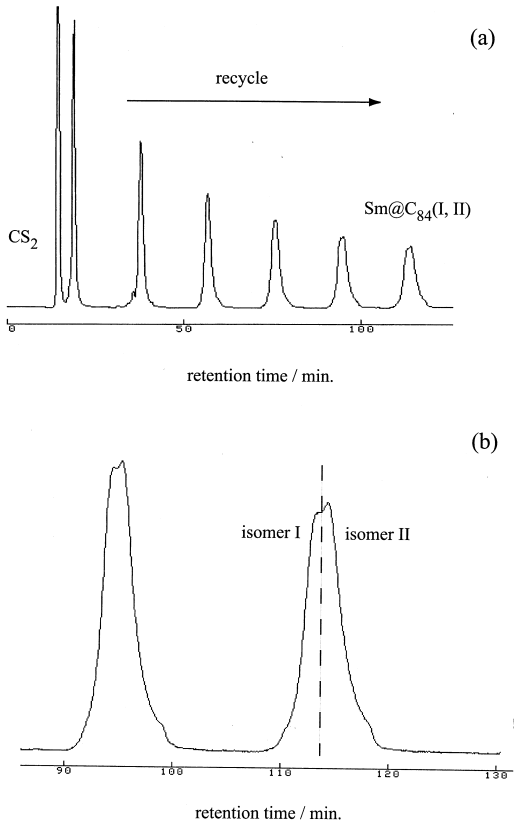

Figure 1. (a) HPLC isolation scheme of the recycling phase for Sm@C_{84}(I, II). (b) Expanded HPLC profile of the 5th and the 6th cycle.

Table 1. The relative abundance of the isolated Sm metallofullerenes[a]

$Sm@C_{74}$	$Sm@C_{76}$(I)	$Sm@C_{76}$(II)	$Sm@C_{78}$	$Sm@C_{80}$	$Sm@C_{82}$(I)
1	0.2	0.1	0.4	0.7	0.3
$Sm@C_{82}$(II)	$Sm@C_{82}$(III)	$Sm@C_{84}$(I)	$Sm@C_{84}$(II)	$Sm@C_{84}$(III)	
1	0.3	0.5	0.5	1	

[a]The values presented here are rough estimates and strongly depend on the experimental conditions.

~500 and 700 nm, whereas for isomer II this region is relatively poor in features.

The absorption spectrum of $Sm@C_{78}$ is shown in Figure 2a. This spectrum is characterized by sharp absorption peaks at ~650 and 800 nm, and a broad feature at ~2200 nm. The onset of the absorption spectrum of a fullerene should be a good measure for the band gap energy of the fullerene. For $Sm@C_{78}$, the onset of the absorption spectrum is ~2600 nm, which corresponds to a band gap of only ~0.5 eV.

There is a close similarity between the absorption spectrum of $Sm@C_{80}$ and those of $M@C_{80}$ (M = Ca, Sr, and Ba) (Figure 2b).[18,19] These spectra appear at ~1400 nm and show a set of distinct peaks at ~500, 600, and 700 nm, and a broad band at ~1100 nm. The similarity strongly suggests that these four kinds of atoms are trapped within the same structural isomer with the same oxidation state.

A similar tendency is also observed with $Sm@C_{82}$. Figure 2c shows the absorption spectra of three isomers of $Sm@C_{82}$. The characteristic feature of the absorption spectra of $Sm@C_{82}$(I, II, III) are almost the same as those of the corresponding isomers of $Ca@C_{82}$(I, III, IV) and $Tm@C_{82}$(B, A, C), respectively.[14,15,19] For example, the absorption spectra of $Sm@C_{82}$(II), $Ca@C_{82}$(III), and $Tm@C_{82}$(A) show a characteristic band near 1200 nm. Since $Ca@C_{82}$(III) has C_2 symmetry based on ^{13}C NMR measurements,[19] $Sm@C_{82}$(II) may also have C_2 symmetry.

Figure 2d shows the absorption spectra of $Sm@C_{84}$(I, II, III). The absorption spectra of $Sm@C_{84}$(I, II) are quite similar to those of the corresponding isomers of $Ca@C_{84}$(I, II), respectively.[15,19] Such a spectroscopic similarity was also observed in the absorption spectra of $Sm@C_{84}$(I, II). At present, it is not clear whether this difference can be ascribed to the structural difference of fullerene cage or to the distinct atom position inside the same cage. On the other hand, the absorption spectrum of $Sm@C_{84}$(III) has quite different features from those of $Sm@C_{84}$(I, II). For example, $Sm@C_{84}$(III) shows a broad band at ~1600 nm, whereas the spectra of $Sm@C_{84}$(I, II) is quite featureless in this region. The structures of $Sm@C_{84}$(I, II) might be very similar to each other, while $Sm@C_{84}$(III) has a different structure from the other two isomers (I, II).

Sm metallofullrenes exhibited a couple of important differences in the number of isomers compared with that of Ca metallofullerenes.[15,19] First, $Ca@C_{82}$ has four isomers, whereas $Sm@C_{82}$ (and $Tm@C_{82}$) has three isomers.[14] The Sm metallofullerene corresponding to $Ca@C_{82}$(II) was not found in this study. Moreover, for C_{84}-based metallofullrenes, $Sm@C_{84}$ has three isomers, although $Ca@C_{84}$ has two isomers.[15,19] A $Ca@C_{84}$ isomer corresponding to $Sm@C_{84}$(III) was not found in the previous study.[15,19] This delicate (and yet important) dependence on the structural isomers of metallofullerenes may be a crucial factor in elucidating the formation mechanism of metallofullerenes.

Electron Energy-Loss Spectroscopy (EELS)

High-energy spectroscopic methods such as X-ray absorption spectroscopy (XAS) and EELS can provide direct proof of the valency of lanthanide ions.[21,22] The valence state of the encaged atom in metallofullerenes has been investigated by these methods.[23–30] In particular, EELS is a powerful method to investigate the electronic properties of metallofullerenes because it can be performed in an electron microscope by using a tiny incident electron beam (typically a nanometer in size) and therefore requires only a small amount of specimen.[9] Figure 3 shows the EELS spectra of a series of Sm metallofullerenes in the M_{45} edges region of Sm. A reference spectrum for a trivalent Sm^{3+} in Sm_2O_3 is also shown at the bottom of Figure 3. The M_{45} spectra consist of two well-separated line groups due to the strong spin–orbit interaction (M_5: $3d_{5/2}\rightarrow 4f_{7/2}$, M_4: $3d_{3/2}\rightarrow 4f_{5/2}$).[21,22] These lines are dominated by the $3d^{10}4f^n\rightarrow 3d^9 4f^{n+1}$ dipole transition and therefore reflect the $4f$ unoccupied density of states. The trivalent Sm^{3+} atom has an electronic configuration of $4f^5$ while that of the divalent Sm^{2+} is $4f^6$. This difference in the electronic state causes the 2~3 eV shifts in energy between the M_{45} peaks of Sm^{3+} and Sm^{2+}[21,22]

The M_{45} edges of all the Sm-containing metallofullerenes currently studied appeared at the same energy positions within the experimental accuracy (~1 eV) (Figure 3). The highest positions for the M_{45} edges were observed at ~1105 and ~1078 eV. Apparently, these positions are shifted to the lower energy region in comparison with those of trivalent Sm^{3+} in Sm_2O_3 (the bottom spectrum in Figure 3). The shift value of the M_5 edge is ~2.1–2.4 eV, which is almost identical to that observed for the XAS spectra of Sm^{2+} and Sm^{3+}.[21,22] In addition, the EELS spectra are very similar in shape to the XAS spectrum reported for a divalent Sm^{2+} in $Sm_{0.3}Y_{0.7}S$.[21] For example, the EELS spectra of Sm metallofullerenes show characteristic M_5 peaks at ~1078 and ~1081 eV, which are similar to those of Sm^{2+} observed for the XAS of $Sm_{0.3}Y_{0.7}S$. Therefore, we can unambiguously conclude that the Sm atom is divalent in $Sm@C_{2n}$ [2n = 74, 78, 80, 82(I, II, III), 84(I, II, III)]. In the following, we will discuss the cage effect on the electronic state of metallofullerenes by using a simple thermochemical cycle model.

A Thermochemical Cycle Model

The present results reveal that the Sm atom prefers to take +2 oxidation state in the fullerene cages [$Sm^{2+}@C_{2n}{}^{2-}$; 2n = 74, 78, 80, 82(I, II, III), 84(I, II, III)]. On the other hand, group 3 and most of the lanthanide metallofullerenes generally take +3 states in the fullerenes.[4,8,9,13,23,24,26,29] The preferential valency is, of course, reflected in a larger stability of the molecule. Here we will interpret this cage size effect on the valency of the Sm ion within a framework of the relative stability of the two

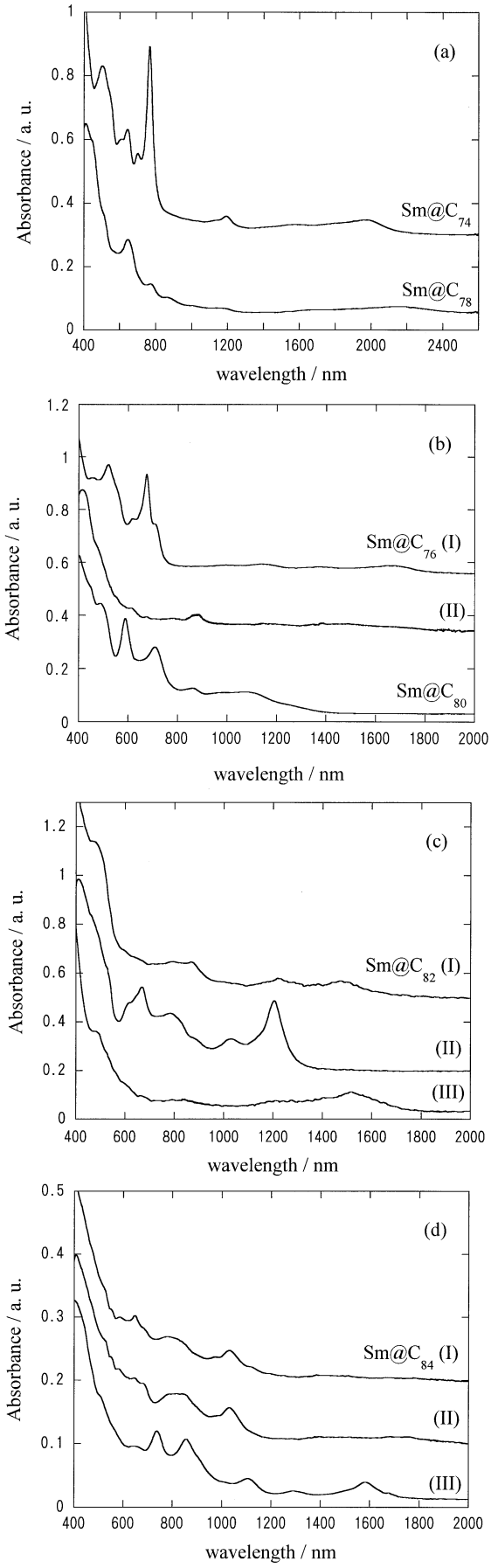

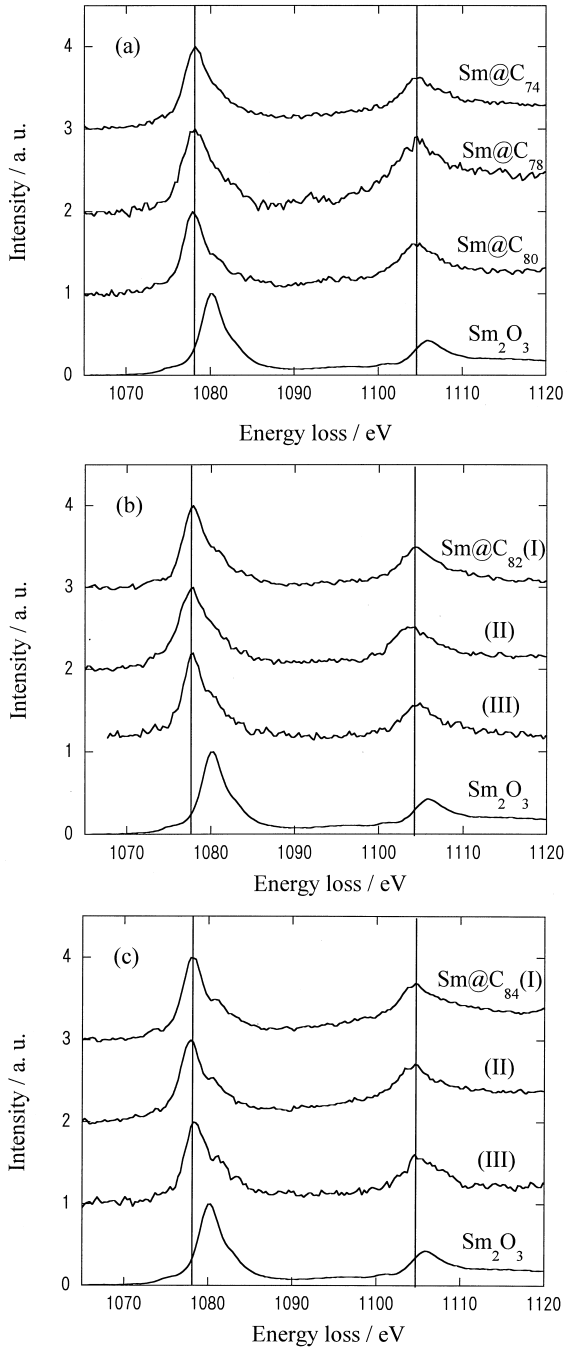

Figure 3. EELS spectra of the Sm-containing metallofullrenes and trivalent Sm^{3+} in Sm_2O_3: (a) $Sm@C_{74}$, $Sm@C_{78}$ and $Sm@C_{80}$; (b) $Sm@C_{82}$(I, II, III); (c) $Sm@C_{84}$(I, II, III).

electronic states ($Sm^{2+}@C_{2n}{}^{2-}$ and $Sm^{3+}@C_{2n}{}^{3-}$) by using a simple thermochemical cycle model (Figure 4).

This thermochemical cycle model is similar to a model previously proposed by Wang et al.[31] In the first step of the

Figure 2. Absorption spectra of the isolated Sm-containing metallofullrenes: (a) $Sm@C_{74}$ and $Sm@C_{78}$; (b) $Sm@C_{76}$(I, II) and $Sm@C_{80}$; (c) $Sm@C_{82}$(I, II, III); (d) $Sm@C_{84}$(I, II, III) in CS_2.

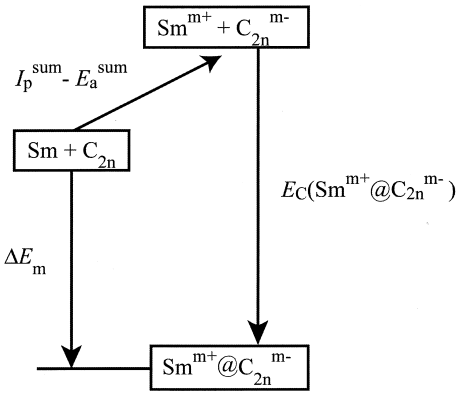

Figure 4. A thermochemical cycle model used to estimate the stabilization energy ΔE_m for Sm@C_{2n} endohedral complexes.

thermochemical cycle (Figure 4), the Sm metal atom emits electrons and becomes the Sm^{m+} state, where m is the valence of Sm ion. This step requires activation energies corresponding to the sum of the ionization potentials of the Sm atom [$I_p^{sum} = I_p(Sm^+) + I_p(Sm^{2+}) + \ldots + I_p(Sm^{m+})$]. In the next step of the cycle, the electron, when transferred to the fullerene cage, releases the energy given by the sum of the corresponding electron affinity [$E_a^{sum} = E_a(C_{2n}^-) + E_a(C_{2n}^{2-}) + \ldots + E_a(C_{2n}^{m-})$]. Finally, the metallofullerene is further stabilized by a Coulomb attraction between the positive ion and the negative fullerene cage [$E_C(Sm^{m+}@C_{2n}^{m-})$]. Hence the stabilization energies, ΔE_m, during the formation of $Sm^{2+}@C_{2n}^{2-}$ (ΔE_2) and $Sm^{3+}@C_{2n}^{3-}$ (ΔE_3) are expressed as

$$\Delta E_2 = I_p(SM^+) + I_p(Sm^{2+}) - E_a(C_{2n}^- - E_a(C_{2n}^{2-}) + E_c(Sm^{2+}@C_{2n}^{2-}), \quad (1)$$

$$\Delta E_3 = I_p(Sm^+) + I_p(Sm^{2+}) + I_p(Sm^{3+}) - E_a(C_{2n}^-) - E_a(C_{2n}^{2-}) - E_a(C_{2n}^{3-}) \quad (2)$$

The relative stability between $Sm^{2+}@C_{2n}^{2-}$ and $Sm^{3+}@C_{2n}^{3-}$ ($\Delta E_{2\to3}$) is thus given by

$$\Delta E_{2\to3} = I_p(Sm^{3+}) - E_a(C_{2n}^{3-}) + \Delta E_C, \quad (3)$$

where $\Delta E_C = E_C(Sm^{3+}@C_{2n}^{3-}) - E_C(Sm^{2+}@C_{2n}^{2-})$.

Precise experimental data exist for $I_p(Sm^{3+})$ (=23.4 eV),[32] whereas no reliable experimental values are available for $E_a(C_{2n}^{3-})$ of the large fullerenes. Hence, we estimated this quantity from the energy level of the lowest unoccupied molecular orbital (LUMO) of C_{2n}^{2-} (Koopman's theorem) by a semi-empirical calculation. Figure 5 shows the optimized structure of C_{2n}^{2-} at the PM3 level. The symmetries of the fullerene cages in Sm@C_{74} and one of Sm@C_{82} can be estimated to be D_{3h} and C_2, respectively (see above). Such structural information on Sm@C_{78}, Sm@C_{80}, and Sm@C_{84} has been limited so far. Hence, in this calculation, we assumed that the symmetries of Sm@C_{78}, Sm@C_{80}, and Sm@C_{84} cages are the same as those of the most abundant isolated hollow fullerenes C_{2v}-C_{78}, D_2-C_{80} and D_2-C_{84}, respectively.[33–36] This assumption can be a good approximation for a qualitative understanding even if the fullerene cages of metallofullerenes generally have different symmetries from those of the corresponding hollow fullerenes.[37,38] All calculations were carried out with the restricted Hartree-Fock (RHF) method. The singlet spin state for each C_{2n}^{2-} was assumed. The obtained $E_a(C_{2n}^{3-})$ values are negative because of the Coulomb repulsion between the electron and the charged cage (Table 2). In Figure 6, the $-E_a(C_{2n}^{3-})$ values are presented as a function of the number of the carbon atoms in the fullerene cage. As a general trend, the $-E_a(C_{2n}^{3-})$ values decrease as the size of the fullerene increases. This implies that the larger fullerene is a better electron accepter than the smaller one.

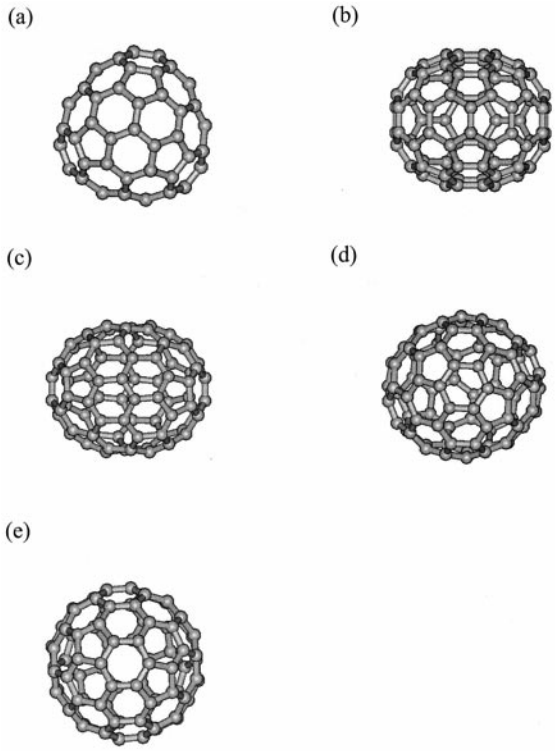

Figure 5. The optimized structures of: (a) D_{3h}-C_{74}^{2-}; (b) C_{2v}-C_{78}^{2-}; (c) D_2-C_{80}^{2-}; (d) C_2-C_{82}^{2-}; and (e) D_2-C_{84}^{2-}. All calculations were carried out at PM3 level.

The main part of the stabilization energy comes from the Coulomb attraction. We estimated this quantity by using a simple spherical shell model.[10] In this model, the metal atom and the fullerene cage are expressed as spheres with radii of *r*

Table 2. The calculated third electron affinities ($E_a(C_{2n}^{3-})$), the Coulomb interactions (ΔE_C) of various fullerene cages (C_{2n}), and the sum of the third electron affinity and the Coulomb interaction ($E_s = -E_a(C_{2n}^{3-}) + \Delta E_C$)

2n	$E_a(C_{2n}^{3-})$/eV	ΔE_C/eV	E_s/eV
74	−2.5 (D_{3h}[a])	−18.1	−15.6
78	−2.4 (C_{2v}[a])	−17.7	−15.3
80	−2.2 (D_2[a])	−17.4	−15.2
82	−1.9 (C_2[a])	−17.2	−15.3
84	−1.7 (D_2[a])	−16.9	−15.2

[a]The symmetry of the calculated isomers.

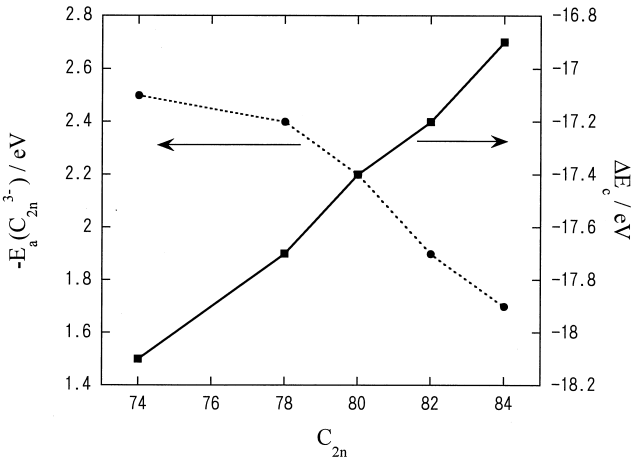

Figure 6. The cage size effects on the estimated third electron affinities [$E_a(C_{2n}{}^{3-})$, solid circles] and the Coulomb interactions (ΔE_C, solid squares).

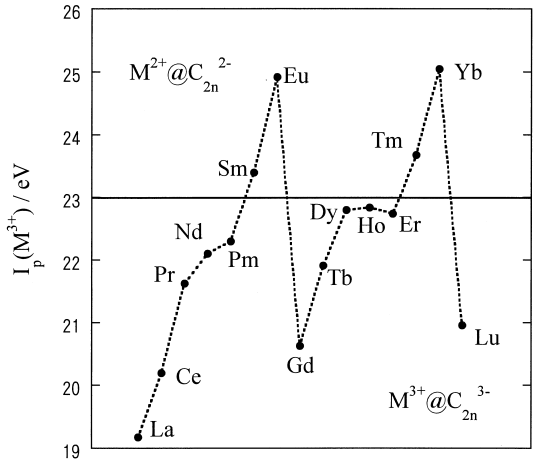

Figure 7. The third ionization potentials [$I_p(M^{3+})$] of the lanthanide elements.

and R, respectively. The Coulomb interaction is given by $E_C(Sm^{m+}@C_{2n}{}^{m-}) = -m^2e^2/4\pi\epsilon_0 R$, where ϵ_0 is a dielectronic constant. The energy difference between E_C of $Sm^{2+}@C_{2n}{}^{2-}$ and $Sm^{3+}@C_{2n}{}^{3-}$ can, therefore, be expressed as $\Delta E_C = -5e^2/4\pi\epsilon_0 R$. By using the calculated R,[10] ΔE_C was obtained for various sizes of fullerene cages from C_{74} to C_{84} (Table 2). These calculations indicate that the ΔE_C value increases during the $+2 \rightarrow +3$ charge transfer process as the radius of the fullerene cage increases (Figure 6).

The Cage Size Effect on the Oxidation State of the Encapsulated Sm Atom

The cage size effect on the relative stability between the two electronic states ($Sm^{2+}@C_{2n}{}^{2-}$ and $Sm^{3+}@C_{2n}{}^{3-}$) should appear in the third electron affinity of the cage [$E_a(C_{2n}{}^{3-})$] and the Coulomb interaction (ΔE_C). Table 2 also shows the sum of these energies ($E_s = -E_a(C_{2n}{}^{3-}) + \Delta E_C$) for each fullerene cage. As stated in the previous section, the stabilization energy from the Coulomb attraction (ΔE_C) becomes larger as the cage size decrease, whereas $-E_a(C_{2n}{}^{3-})$ exhibits an opposite trend (Figure 6). Consequently, E_s will not become a sensitive function of the fullerene cage size.

It has been revealed that there is a correlation between $I_p(M^{3+})$ of the encapsulated metal and its oxidation state in a fullerene cage (Figure 7).[39] The solid line at ~23 eV denotes a threshold. The atoms above this threshold prefer to take +2 oxidation states in the fullerene cages (group B) because a relatively high energy is needed to have +3 states,[4,8,10,12,14–20,27,28,30] whereas the atoms below the threshold take +3 states inside the fullerenes (group A).[4,8,9,13,23,24,26,29] The energetic difference between $I_p(M^{3+})$ of these groups is 0.58 eV [$= I_p(Sm^{3+}) - I_p(Ho^{3+})$], which exceeds the difference between the largest and the smallest E_s estimated above (~0.4 eV). This result implies that the oxidation states of the Sm ions do not change in the fullerene cages from C_{74} to C_{84}.

Recently, we have also carried out similar EELS measurements on a series of Sc di-metallofullerenes ($Sc_2@C_{2n}$, 2n = ~80–90).[40] The observed peak position of the Sc L edge is found to be almost identical to these molecules. Although the valency of the Sc atom in $Sc_2@C_{84}$ is still controversial,[41] these results indicate that the Sc atoms are trapped within the fullerenes with the same oxidation state. On this basis, we can conclude that the fullerene cage size effect on the electronic states of the encapsulated metal atoms is generally rather small.

The above simple model can explain the present experimental observation that the oxidation state of Sm atom is insensitive to the fullerene cage. We should note, however, that this model provides us with a qualitative understanding of the experimental results. For example, we cannot explain that group A atoms take +3 state in fullerenes by this model, i.e., $\Delta E_{2\rightarrow 3}$ of these metallofullerenes have positive values. This discrepancy may be due to energy uncertainties for the individual steps described earlier. The values of $E_a(C_{2n}{}^{3-})$ calculated here, for example, may be underestimated because it is well-known that Koopman's theorem provides a smaller E_a than the true value. Moreover, in a realistic description, the encapsulated metal atom does not locate at the center of the cage. Theoretical calculations[42,43] have shown that there is ~2–3 eV of the energy gain from the off-center location in $Sc@C_{82}$ and $La@C_{82}$. A more detailed theoretical study is required to quantitatively describe the electron transfer process in the methallofullerenes.

CONCLUSION

We have reported the first isolation of a series of Sm-containing metallofullerenes, $Sm@C_{74}$, $Sm@C_{76}$ (I, II), $Sm@C_{78}$, $Sm@C_{80}$, $Sm@C_{82}$ (I, II, III), and $Sm@C_{84}$ (I, II, III), and their characterization by UV-vis-NIR absorption spectroscopy. The UV-Vis-NIR absorption spectra of $Sm@C_{74}$, $Sm@C_{80}$, $Sm@C_{82}$ (I, II, III), and $Sm@C_{84}$ (I, II) are quite similar to those of the corresponding Ca, Sr, Ba, Eu, Tm, and Yb-based metallofullerenes. In contrast, the absorption spectra of $Sm@C_{76}$(I, II), $Sm@C_{78}$, and $Sm@C_{84}$(III) show a novel feature: the onset for $Sm@C_{78}$ is observed to be ~2600 nm, which corresponds to a small band gap (~0.5 eV). The oxidation states of the Sm atom in Sm-containing metallofullerenes [$Sm@C_{74}$, $Sm@C_{78}$, $Sm@C_{80}$, $Sm@C_{82}$ (I, II, III), and $Sm@C_{84}$ (I, II, III)] are investigated by EELS, which reveals

that the Sm atom takes a +2 oxidation state in the fullerene cages.

REFERENCES

1 Osawa, E. Chouhoukouzoku. *Kagaku* 1970, **25**, 850–863 (in Japanese)
2 Kroto, H.W., Heath, J.R., O'Brien, S.C., Curl, R.F., and Smalley, R.E. Buckminsterfullerene. *Nature.* 1985, **318**, 162–163
3 Krätschmer, W., Lamb, L.D., Fostiropoulos, K., and Huffman, D.R. Solid C_{60}: A new form of carbon. *Nature.* 1990, **347**, 354–358
4 Shinohara, H. Endohedral metallofullerene. *Rep. Prog. Phys.* 2000, **63**, 843–892
5 Lian, Y.F., Shi, Z.J., Zhou, X.H., He, X.R., and Gu, Z.N. High-yield synthesis of endohedral metallofullerenes $Y@C_{2n}$ and $Y_2@C_{2n}$. *Chin. Chem. Lett.* 1999, **10**, 425–428
6 Lian, Y., Shi, Z., Zhou, X., He, X., Gu, Z. Preparation and enrichment of Samarium endohedral fullerenes. *Chem. Mater.* 2001, **13,** 39–42
7 Lian, Y., Shi, Z., Zhou, X., He, X., Gu, Z. *Carbon* submitted
8 Shinohara, H. Shedding more light on metallofullerenes. In: *Fullerenes, Recent Advances in the Chemistry and Physics of Fullerenes and Related Materials, vol. 4*, Kadish, K.M., Ruoff, R.S., Eds., The Electrochemical Society, Pennington, NJ, 1997, 467–474
9 Suenaga, K., Iijima, S., Kato, H., and Shinohara, H. Fine-structure analysis of Gd M_{45} near-edge EELS on the valence state of $Gd@C_{82}$ microcrystals. *Phys. Rev. B.* 2000, **62**, 1627–1630
10 Okazaki, T., Suenaga, K., Lian, Y., Gu, Z. and Shinohara, H. Direct EELS observation of the oxidation states of Sm atoms in $Sm@C_{2n}$ metallofullerenes ($74 \leq 2n \leq 84$), *J. Chem. Phys.* 2000, **113,** 9593–9597
11 Frisch, M.J., Trucks, G.W., Schlegel, H.B., Gill, P.M.W., Johnson, B.G., Bobb, M.A., Cheeseman, J.R., Keith, T., Petersson, G.A., Montgomery, G.A., Raghavachari, K., Al-Laham, M.A., Zakrzewski, V.G., Ortiz, J.V., Foresman, J.B., Cioslowski, J., Stefanov, B.B., Nanayakkara, A., Challacombe, M., Peng, C.Y., Ayala, P.Y., Chen, W., Wong, M.W., Andres, J.L., Replogle, E.S., Gomperts, R., Martin, R.L., Fox, D.L., Binkley, J.S., DeFrees, D.J., Baker, J., Stewart, J. P., Head-Gordon, M., Gonzalez, C., and Pople, J.A. *Gaussian 98W*. Gaussian Inc., Pittsburgh, PA, 1998
12 Okazaki, T., Lian, Y., Gu, Z., Suenaga, K., and Shinohara, H. Isolation and spectroscopic characterization of Sm-containing metallofullerenes. *Chem. Phys. Lett.* 2000, **320**, 435–440
13 Sueki, K., Akiyama, K., Kikuchi, K., and Nakahara, H. Specificity of carbon cages towards oxidation states of metal atoms in metallofullerenes. *Chem. Phys. Lett.* 1998, **291**, 37–43
14 Kirbach, U., and Dunsch, L. The existence of stable $Tm@C_{82}$ isomers. *Angew. Chem. Int. Ed. Engl.* 1996, **35**, 2380–2383
15 Xu, Z., Nakane, T., and Shinohara, H. Production and isolation of $Ca@C_{82}$(I-IV) and $Ca@C_{84}$(I, II) metallofullerenes. *J. Am. Chem. Soc.* 1996, **118**, 11309–11310
16 Dennis, T.J.S., and Shinohara, H. Production and isolation of endohedral strontium- and barium-based monometallofullerenes: Sr/Ba@C_{82} and Sr/Ba@C_{84}. *Chem. Phys. Lett.* 1997, **278**, 107–110
17 Wan, T.S.M., Zhang, H.-W., Nakane, T., Xu, Z., Inakuma, M., Shinohara, H., Kobayashi, K. and Nagase, S. Production, isolation, and electronic properties of missing fullerenes: $Ca@C_{72}$ and $Ca@C_{74}$. *J. Am. Chem. Soc.* 1998, **120**, 6806–6807
18 Dennis, T.J.S., and Shinohara, H. Production and isolation of the C_{80}-based group 2 *incar*-fullerenes: *i*CaC_{80}, *i*SrC_{80} and *i*BaC_{80}. *Chem. Commun.* 1998, 883–884
19 Dennis, T.J.S., and Shinohara, H. Production, isolation, and characterization of group-2 metal-containing endohedral metallofullerenes. *Appl. Phys. A* 1998, **66**, 243–247
20 Kuran, P., Krause, M., Bartl, A., and Dunsch, L. Preparation, isolation and characterization of $Eu@C_{74}$: the first isolated europium endohedral fullerene. *Chem. Phys. Lett.* 1998, **292**, 580–586
21 Kaindl, G., Kalkowski, G., Brewer, W.D., Perscheid, B., and Holtzberg, F. *M*-edge x-ray absorption spectroscopy of 4*f* instabilities in rare-earth systems. *J. Appl. Phys.* 1984, **55**, 1910–1915
22 Thole, B.T., van der Laan, G., Fuggle, J.C., Sawatzky, G.A., Karnatak, R.C., and Esteva, J.-M. 3*d* x-ray-absorption lines and the $3d^{9}4f^{n+1}$ multiplets of the lanthanides. *Phys. Rev. B.* 1985, **32**, 5107–5118
23 Hino, S., Takahashi, H., Iwasaki, K., Matsumoto, K., Miyazaki, T., Hasegawa, S., Kikuchi, K., and Achiba, Y. Electronic structure of metallofullerenes LaC_{82}: Electron transfer from lanthanum to C_{82}. *Phys. Rev. Lett.* 1993, **71**, 4261–4263
24 Poirier, M.D., Knupfer, M., Weaver, J.H., Andreoni, W., Laasonen, K., Parrinello, M., Bethune, D.S., Kikuchi, K., and Achiba, Y. Electronic and geometric structure of LaC_{82} and C_{82}: Theory and experiment. *Phys. Rev. B* 1994, **49**, 17403–17412
25 Takahashi, T., Ito, A., Inakuma, M., and Shinohara, H. Divalent scandium atoms in the cage of C_{84}. *Phys. Rev. B* 1995, **52**, 13812–13814
26 Hino, S., Umishita, K., Iwasaki, K., Miyazaki, T., Miyake, T., Kikuchi, K., and Achiba, Y. Photoelectron spectra of metallofullerenes, GdC_{82} and La_2C_{80}: Electron transfer from the metal to the cage. *Chem. Phys. Lett.* 1997, **281**, 115–122
27 Pichler, T., Golden, M.S., Knupfer, M., Fink, J., Kirbach, U., Kuran, P., and Dunsch, L. Monometallofullerene $Tm@C_{82}$: proof of an encapsulated divalent Tm ion by high-energy spectroscopy. *Phys. Rev. Lett.* 1997, **79**, 3026–3029
28 Umishita, K., Iwasaki, K., Hino, S., Aoki, M., Kobayashi, K., Nagase, S., Dennis, T.J.S., Nakane, T., and Shinohara, H. Utraviolet photoelectron spectra of $Ca@C_{82}$. *Proceedings of the 16th Fullerene General Symposium* 1999, 83–84
29 Giefers, H., Nessel, F., Györy, S.I., Strecker, M., Wortmann, G., Grushko, Yu. S., Alekseev, E.G., and Kozlov, V.S. Gd-L_{III} EXAFS study of structural and dynamic properties of $Gd@C_{82}$ between 10 and 300 K. *Carbon* 1999, **37**, 721–725
30 Inoue, T., Kubozono, Y., Kashino, S., Takabayashi, Y., Fujitaka, K., Hida, M., Inoue, M., Kanbara, T., Emura, S., and Uruga, T. Electronic structure of $Eu@C_{60}$ studied by XANES and UV-VIS absorption spectra. *Chem. Phys. Lett.* 2000, **316**, 381–386

31 Wang, Y., Tománek, D., and Ruoff, R.S. Stability of $M@C_{60}$ endohedral complexes. *Chem. Phys. Lett.* 1993, **208**, 79–85
32 CRC Handbook of Chemistry and Physics, 80th ed.; CRC press: Boca Raton, 1999
33 Diederich, F., Whetten, R.L., Thilgen, C., Ettl, R., Chao, I., and Alvarez, M.M. Fullerene isomerism: isolation of C_{2v}-C_{78} and D_3-C_{78}. *Science.* 1991, **254**, 1768–1770
34 Kikuchi, K., Nakahara, N., Wakabayashi, T., Suzuki, S., Shiromaru, H., Miyake, Y., Saito, K., Ikemoto, I., Kainosho, M., and Achiba, Y. NMR characteriztion of isomers of C_{78}, C_{82} and C_{84} fullerenes. *Nature.* 1992, **357**, 142–145
35 Wang, C.-R., Sugai, T., Kai, T., Tomiyama, T., and Shinohara, H. Production and isolation of an ellipsoidal C_{80} fullerene. *Chem. Comm.* 2000, 557–558
36 Dennis, T.J.S., Kai, T., Asato, K., Tomiyama, T., Shinohara, H., Yoshida, T., Kobayashi, Y., Ishiwatari, H., Miyake, Y., Kikuchi, K., and Achiba, Y. Isolation and characterization by ^{13}C NMR spectroscopy of [84]fullerene minor isomers. *J. Phys. Chem. A* 1999, **103**, 8747–8752
37 Takata, M., Nishibori, E., Umeda, B., Sakata, M., Yamamoto, E., and Shinohara, H. Structure of endohedral dimetallofullerene $Sc_2@C_{84}$. *Phys. Rev. Lett.* 1997, **78**, 3330–3333
38 Takata, M., Nishibori, E., Umeda, B., Sakata, M., Inakuma, M., Yamamoto, E. and Shinohara, H. Triangle scandium cluster imprisoned in a fullerene cage. *Phys. Rev. Lett.* 1999, **83**, 2214–2217
39 Huang, H., and Yang, S. Relative yields of endohedral lanthanide metallofullerenes by arc synthesis and their correlation with the elution behavior. *J. Phys. Chem. B* 1998, **102**, 10196–10200
40 Okazaki, T., Wang, C.-R., Suenaga, K., and Shinohara, H. in preparation.
41 Pichler, T., Hu, Z., Grazioli, C., Legner, S., Knupfer, M., Golden, M.S., Fink, J., de Groot, F.M.F., Hunt, M.R.C., Rudolf, P., Follath, R., Jung, Ch., Kjeldgaard, L., Brühwiler, P., Inakuma, M., and Shinohara, H. Proof for trivalent Sc ion in $Sc_2@C_{84}$ from high-energy spectroscopy. *Phys. Rev. B* 2000, **62,** 13196–13201
42 Nagase, S., and Kobayashi, K. Metallofullerenes MC_{82} (M=Sc, Y, and La). A theoretical study of the electronic and structural aspects. *Chem. Phys. Lett.* 1993, **214**, 57–63
43 Nagase, S., and Kobayashi, K. Theoretical study of the lanthanide fullerene CeC_{82}. comparison with ScC_{82}, YC_{82} and LaC_{82}. *Chem. Phys. Lett.* 1994, **228**, 106–110